Available online at www.sciencedirect.com
SCIENCE DIRECT®
Journal of Organometallic Chemistry 685 (2003) 156–161
Journal of Organometallic Chemistry
www.elsevier.com/locate/jorganchem

Structure and oxidation of octakis(*tert*-butyldimethylsilyl)octasilacubane

Masafumi Unno [a], Takayoshi Matsumoto [a], Kikuo Mochizuki [a], Koichi Higuchi [a], Midori Goto [b], Hideyuki Matsumoto [a,*]

[a] *Department of Nano-Material Systems, Graduate School of Engineering, Gunma University, Kiryu 376-8515, Japan*
[b] *National Institute of Materials and Chemical Research, Tsukuba, Ibaraki 305-8565, Japan*

Received 17 March 2003; received in revised form 9 April 2003; accepted 15 April 2003

Abstract

The molecular structure of the silyl-substituted octasilacubane $[(t\text{-BuMe}_2\text{Si})\text{Si}]_8$ (**1**) was analyzed by X-ray crystallography, and the structural parameters (bond length and angles) were compared with those of the alkyl- and aryl-substituted octasilacubanes. A thermogravimetric analysis revealed that **1** remained stable under argon up to 300 °C, indicating that **1** is much more thermally stable than alkyl-substituted $(\text{ThexSi})_8$ (Thex = 1,1,2-trimethylpropyl) (**2**), which decomposed at 200 °C. Although compound **1** is stable in the air, **1** reacted with *m*-chloroperoxybenzoic acid (*m*CPBA). Thus, treatment of **1** with fourteen equivalents of *m*CPBA led to the formation of octakis(*tert*-butyldimethylsilylsilsesquioxane) (**3**) in 98% yield. The structure of **3** was also established by X-ray crystallography, indicating that all the oxygen atoms inserted into the Si–Si bonds of the Si_8 framework and the exocyclic Si–Si bonds remained intact under the conditions employed. Compound **3** is the first example of silsesquioxane with bulky silyl substituents, and shows relatively intense absorptions in the UV region.

Keywords: Polysilane; Octasilacubane; Crystal structure; Octasilsesquioxane; Oxidation of polysilane

1. Introduction

Octasilacubanes are intriguing polyhedral polysilanes because of their unique electronic properties arising from their highly strained Si–Si σ-bonded framework [1]. Since the synthesis of the silyl-substituted octasilacubane $[(t\text{-BuMe}_2\text{Si})\text{Si}]_8$ (**1**) in 1988 [2], and the alkyl-substituted one $(\text{ThexSi})_8$ (Thex = 1,1,2-trimethylpropyl) (**2**) in 1992 [3], we have been interested in the chemistry of these octasilacubanes. Previously, we reported the reaction of **2** with PCl_5 leading to 4,8-dichlorooctathexytetracylo[3.3.0.0^{2,7}.0^{3,6}]octasilane (**4**) via skeletal rearrangement [4], the halogenation of **2** with Br_2 or I_2 leading to 4,8-dibromo- or 4,8-diiodooctathexytetracylo[3.3.0.0^{2,7}.0^{3,6}]octasilane (**5** or **6**), and the reductive dehalogenation of **4**–**6** with sodium to regenerate **2** [5], photo-initiated partial oxidation of **2** with dimethylsulfoxide giving monooxaoctasilahomocubane and dioxaoctasilabishomocubane [6], the photoluminescent property of **2** [7], and photolysis of **2** [8]. Also, as a relevant work, we reported the synthesis, X-ray structure, and reactions of octagermacubane $(\text{ThexGe})_8$ [9]. These reactions are summarized in Scheme 1.

In this paper, we report the following new results: (1) X-ray crystallography of **1**, which enabled us to compare the structural parameters among silyl-, alkyl-, and aryl-substituted octasilacubanes; (2) thermal stability of **1**; (3) the oxidation reaction of **1** with *m*-chloroperoxybenzoic acid (*m*CPBA), giving octakis(*tert*-butyldimethylsilylsilsesquioxane) (**3**).

* Corresponding author. Tel.: +81-277-30-1293; fax: +81-277-30-1291.
E-mail address: matumoto@chem.gunma-u.ac.jp (H. Matsumoto).

0022-328X/03/$ - see front matter © 2003 Elsevier Science B.V. All rights reserved.
doi:10.1016/S0022-328X(03)00288-2

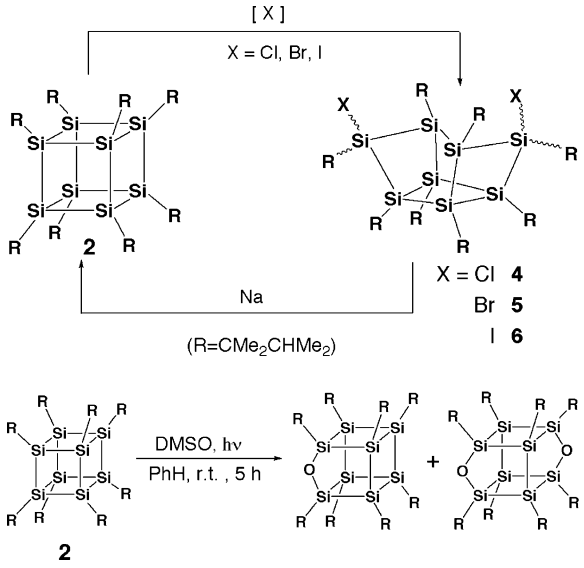

Scheme 1.

2. Results and discussion

2.1. Crystal structure of octakis(tert-butyldimethylsilyl)octasilacubane (1)

Octasilacubane **1** was synthesized in 1988 as the first example of polyhedral compounds comprising Group-14 elements, Si, Ge, and Sn [2]. This compound, however, is very sensitive to X-ray and thus we could not obtain a satisfactory result for structural analysis by X-ray crystallography. Fortunately, recent progress of crystallographic analysis enabled the rapid measurement of such a relatively unstable compound. Thus, reinvestigation of the X-ray analysis was performed, and the structure of **1** was determined successfully. A yellow single crystal suitable for the crystallography was obtained by the recrystallization from methylcyclohexane at room temperature (r.t.). Molecular structure is shown in Fig. 1, and crystallographic data and selected bond lengths and angles are given in Tables 1 and 2. Against the high symmetry of the framework, the crystal structure of **1** showed no symmetry elements. This is explained by assuming that the eight bulky substituents move from the symmetrical positions in order to release the steric hindrance and that the symmetry of the molecule was lost. The Si–Si bond lengths range from 2.396(4) to 2.429(4) Å for the Si_8 framework and 2.370(6)–2.398(4) Å for the exocyclic bonds. Average Si–Si bond lengths of the framework was 2.412(6) Å and this value is slightly less than that of $(ThexSi)_8$ **2** (2.421(2) Å) [3], but somewhat longer than that of $(t\text{-}BuSi)_8$ (2.385(8) Å) [1d] and that of $(2,6\text{-}Et_2C_6H_3Si)_8$ (2.399 Å) [1c]. The Si–Si–Si bond angles of the framework vary from 88.5(1) to 91.8(2)°. The distortion from an ideal cube may be due to the steric hindrance of the silyl substituents.

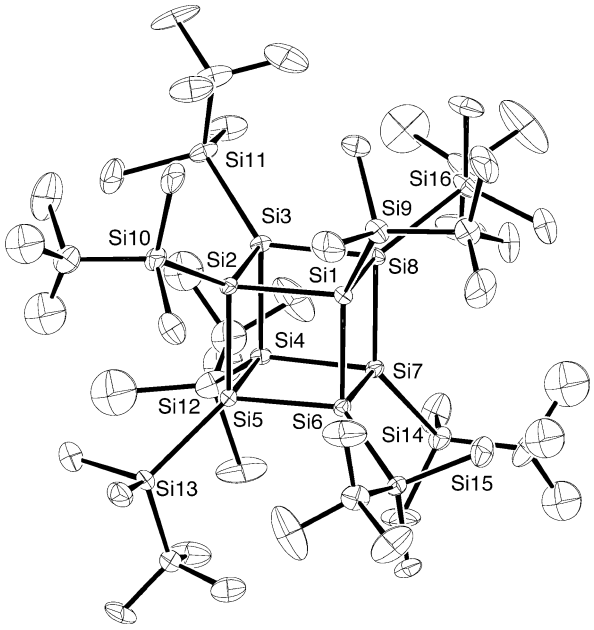

Fig. 1. ORTEP drawing of **1**. Hydrogen atoms were omitted for clarity.

Table 1
Summary of crystal data, data collection, and refinement of **1** and **3**

	1	**3**
Formula	$C_{48}H_{120}Si_{16}$	$C_{48}H_{120}Si_{16}O_{12}$
Molecular weight	1146.8	1338.8
Crystal size (mm)	0.3 × 0.3 × 0.3	0.4 × 0.5 × 0.4
Crystal system	Triclinic	Monoclinic
Space group	$P\bar{1}$	$C2/c$
a (Å)	13.274(3)	22.488(4)
b (Å)	23.347(4)	15.413(1)
c (Å)	13.060(2)	24.301(4)
α (°)	92.241(9)	
β (°)	112.851(7)	100.41(1)
γ (°)	96.77(1)	
V (Å^3)	3687.8(1)	8284.1(19)
Z	2	4
Diffractometer	Rigaku RAXIS-IV	Enraf-Nonius CAD-4
Radiation (λ, Å)	Mo–Kα (0.71070)	Cu–Kα (1.54056)
μ (mm^{-1})	0.303	2.6549
2θ max, (°)	55.1	120
No. of reflns measd	9648	6100
No. of obsd reflns	5209	4991
R	0.091	0.069
R_w	0.092	0.069

2.2. Properties of octasilacubane 1

As mentioned above, the structural parameters of compound **1** are almost same as those of $(ThexSi)_8$ (**2**). There are, however, significant differences in the thermal and kinetic stability between **1** and **2**. A thermogravimetric analysis revealed that the Si_8 framework of **1** is thermodynamically much more stable than **2**. Fig. 2 shows that compound **2** remained stable under argon to 200 °C, after which gradual weight loss occurred, while **1**

Table 2
Selected bond lengths (Å) and angles (°) for **1**

Bond lengths					
Si(1)–Si(2)	2.406(5)	Si(1)–Si(6)	2.396(4)	Si(1)–Si(8)	2.424(5)
Si(1)–Si(9)	2.370(6)	Si(2)–Si(3)	2.413(5)	Si(2)–Si(5)	2.420(4)
Si(2)–Si(10)	2.386(5)	Si(3)–Si(4)	2.429(4)	Si(3)–Si(8)	2.408(6)
Si(3)–Si(11)	2.392(5)	Si(4)–Si(5)	2.406(5)	Si(4)–Si(7)	2.410(6)
Si(4)–Si(12)	2.383(7)	Si(5)–Si(6)	2.411(5)	Si(5)–Si(13)	2.395(4)
Si(6)–Si(7)	2.418(5)	Si(6)–Si(14)	2.381(5)	Si(7)–Si(8)	2.407(4)
Si(7)–Si(15)	2.385(5)	Si(8)–Si(16)	2.398(4)		
Bond angles					
Si(2)–Si(1)–Si(6)	89.4(2)	Si(2)–Si(5)–Si(13)	128.6(2)	Si(2)–Si(1)–Si(8)	91.1(2)
Si(4)–Si(5)–Si(6)	90.9(2)	Si(2)–Si(1)–Si(9)	115.2(2)	Si(4)–Si(5)–Si(13)	121.6(2)
Si(6)–Si(1)–Si(8)	91.8(2)	Si(6)–Si(5)–Si(13)	126.5(2)	Si(6)–Si(1)–Si(9)	140.4(2)
Si(1)–Si(6)–Si(5)	91.1(2)	Si(8)–Si(1)–Si(9)	116.7(2)	Si(1)–Si(6)–Si(7)	88.4(1)
Si(1)–Si(2)–Si(3)	88.9(2)	Si(1)–Si(6)–Si(14)	117.1(2)	Si(1)–Si(2)–Si(5)	90.7(2)
Si(5)–Si(6)–Si(7)	89.0(2)	Si(1)–Si(2)–Si(10)	116.4(2)	Si(5)–Si(6)–Si(14)	131.2(2)
Si(3)–Si(2)–Si(5)	91.4(2)	Si(7)–Si(6)–Si(14)	127.8(2)	Si(3)–Si(2)–Si(10)	138.8(2)
Si(4)–Si(7)–Si(6)	90.7(2)	Si(5)–Si(2)–Si(10)	118.4(2)	Si(4)–Si(7)–Si(8)	89.2(2)
Si(2)–Si(3)–Si(4)	88.5(1)	Si(4)–Si(7)–Si(15)	116.6(2)	Si(2)–Si(3)–Si(8)	91.3(2)
Si(6)–Si(7)–Si(8)	91.7(2)	Si(2)–Si(3)–Si(11)	119.4(2)	Si(6)–Si(7)–Si(15)	119.1(2)
Si(4)–Si(3)–Si(8)	88.8(2)	Si(8)–Si(7)–Si(15)	137.6(2)	Si(4)–Si(3)–Si(11)	127.2(2)
Si(1)–Si(8)–Si(3)	88.6(2)	Si(8)–Si(3)–Si(11)	129.9(2)	Si(1)–Si(8)–Si(7)	88.0(1)
Si(3)–Si(4)–Si(5)	91.3(2)	Si(1)–Si(8)–Si(16)	128.5(2)	Si(3)–Si(4)–Si(7)	90.7(2)
Si(3)–Si(8)–Si(7)	91.2(2)	Si(3)–Si(4)–Si(12)	122.0(2)	Si(3)–Si(8)–Si(16)	128.5(2)
Si(5)–Si(4)–Si(7)	89.3(2)	Si(7)–Si(8)–Si(16)	120.0(2)	Si(5)–Si(4)–Si(12)	126.1(2)
Si(7)–Si(4)–Si(12)	126.8(2)	Si(2)–Si(5)–Si(4)	88.8(1)	Si(2)–Si(5)–Si(6)	88.7(2)

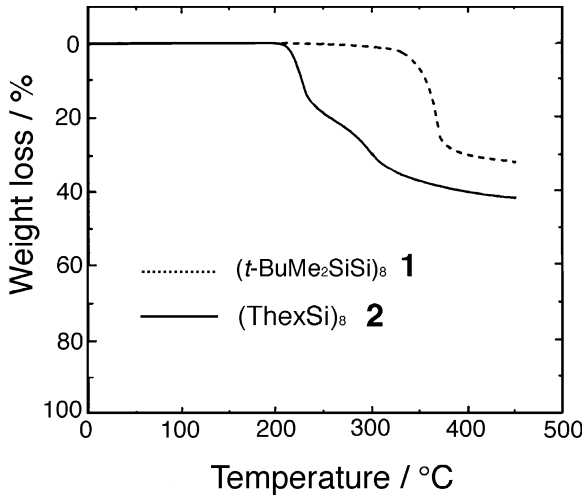

Fig. 2. Thermogravimetric curves of **1** and **2**.

remained stable to 300 °C. The observed trend is in accord with the results of the *ab initio* calculations reported by Nagase, who had predicted that the strain energy of the permethylated octasilacubane $(MeSi)_8$ (88.9 kcal mol^{-1}), is about 10 kcal mol^{-1} more than that of the silyl-substituted derivative $(H_3SiSi)_8$ (77.9 kcal mol^{-1}) [10].

Compound **1** exhibits a higher reactivity towards an electrophile compared to **2**. For example, although the crystals of **1** are infinitely stable in an inert atmosphere, they decompose to a colorless solid for several days in the air at r.t. [3]. By comparison, **2** in crystalline form exhibits no change in color upon exposure to atmosphere for 2 weeks. Furthermore, the Si_8 framework of **1** can be oxidized with peracid. Thus, treatment with fourteen equivalents of *m*CPBA in benzene at r.t. afforded octasilsesquioxane **3** in 98% yield, as colorless crystals (Scheme 2). It should be noted that the further oxidation starting from **3** with ten equivalents of *m*CPBA for 20 days was resulted in the recovery of **3**, and no oxidation of exocyclic Si–Si bonds was observed. In contrast, the peracid oxidation was much slower for the thexyl-substituted octasilacubane **2**, and the reaction resulted in the formation a mixture of the partial oxidation products $(ThexSi)_8O_n$ even under forced conditions [6]. The observed difference in their reactivity can be explained by considering both steric and electronic effects of the substituents. In comparison with thexyl group, *t*-butyldimethylsilyl group is bulkier in size (*t*-Bu vs. *i*-Pr in the terminal), however, longer exocyclic Si–Si bonds (2.370–2.398 Å) over Si–C bonds in thexyl (1.963–1.978 Å) possibly make the oxidation of the framework easier. In addition to this, we also

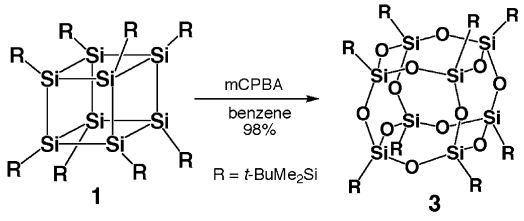

Scheme 2.

attributed the higher reactivity of **1** to the electron-releasing inductive effect of the trialkylsilyl groups [11].

Octasilsesquioxane **3** was characterized by NMR, IR, and mass spectroscopy (Section 3). In the electron impact mass spectrum of **3**, the molecular ion cluster (M^+) was observed in the range 1336–1341, in good agreement with the calculated formula of $C_{48}H_{120}Si_{16}O_{12}$. The ^{1}H-NMR spectrum showed two singlets at δ 0.96 (72H, *t*-Bu) and 0.05 (48H, Me), which were fully consistent with the highly symmetrical structure in the solution. In CP-MAS spectra, anisotropy was observed for substituents; two peaks were observed for Si atom in the substituents (in ^{29}Si-NMR) and dimethyl groups (in ^{13}C-NMR), while in $CDCl_3$, they showed only single peak. Other peaks and the chemical shifts were similar.

2.3. Structure of octakis(*tert*-butyldimethylsilylsilsesquioxane) (*3*)

The structure of **3** was established by spectroscopy and X-ray crystallography. The molecular structure (Fig. 3) indicates that all the oxygen atoms are inserted into the Si–Si bonds of the Si_8 framework and exocyclic Si–Si bonds remained intact under the conditions employed. The experimental detail for X-ray analysis is given in Table 1 and selected bond lengths and angles are listed in Table 3. The Si_8O_{12} framework has C_2 symmetry with the two-hold axis passing through O(6) and O(7). The substituents showed roughly two orientations; *t*-Bu–Si bonds were parallel and perpendicular to the symmetry axis, which explains the two peaks for substituents in CP-MAS NMR. Structural parameters of **3** reflected the steric hindrance compared with those for the reported octasilsesquioxanes [13]. The Si–O bond lengths range between 1.620(7) and 1.630(6) Å (average 1.625 Å), and this value is longer than the other octasilsesquioxanes; average Si–O lengths were 1.604 Å for $(MeOSi)_8O_{12}$ [13b], 1.616 Å for $(PhCH_2Si)_8O_{12}$ [13c], 1.615 Å for $(IC_3H_6Si)_8O_{12}$ [13d], and 1.610 Å for $(i\text{-}PrSi)_8O_{12}$ [13e]. Interestingly, when compared with hexasilsesquioxanes, average Si–O length of **2** is still similar or only slightly longer; for example, 1.619 Å for $(ThexSi)_6O_9$ [12] and 1.625 Å for $(cyclohexyl)_6O_9$. The Si–O–Si bond angles vary from 148.5(4) to 152.2(4)° and average was 150.2°, and also this average value was slightly larger than those in the former cases (average 148.1–148.9°). The silsesquioxane **3** is thermally stable and TGA measurement (25–480 °C, 5 °C min^{-1}) showed no change in weight until the temperature reaches 300 °C (Fig. 4).

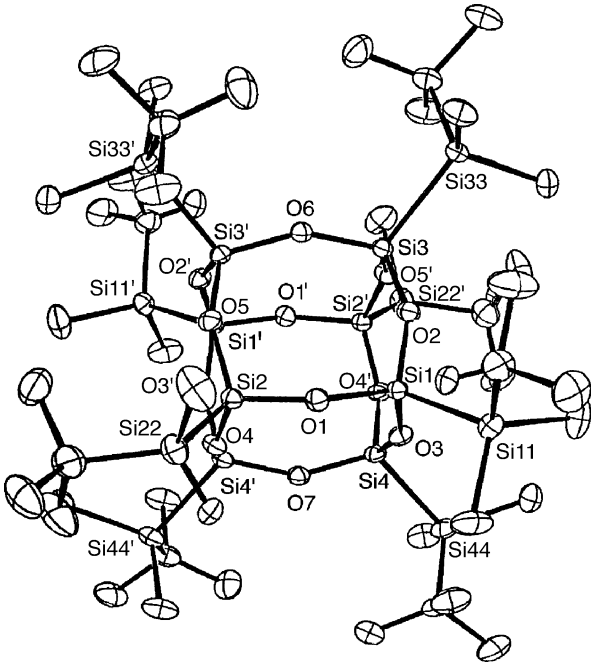

Fig. 3. Molecular drawing of **3**. Hydrogen atoms were omitted for clarity.

Octasilsesquioxane **3** is the first example of T_8 (octasilsesquioxane) with bulky substituents, because conventional hydrolysis-dehydration methods could not give cage products, but incompletely condensed silanols. We reported the synthesis of silsesquioxanes starting from silanols with dicyclohexylcarbodiimide [12], but with this method, only T_6 [$(t\text{-}BuSi)_6O_9$ or $(ThexSi)_6O_9$] was obtained from respecting silanols.

2.4. Physical property (UV spectrum) of *3*

Important to note is the fact that compound **3** exhibits relatively intense absorption in the UV region. As shown in Fig. 5, the lowest transition-energy absorption of **3** in cyclohexane occurs at 285 nm (ε 4900). As **3** has no polysilane chain or ring, multiple Si–Si σ conjugation is not possible. In practice, peralkylated disilanes exhibit the lowest transition-energy absorption around 200 nm [14]. The bathochromic shift of **3** relative to these disilanes is not clearly understood, however, such a property is observed only in this system; interaction of exocyclic Si–Si bonds may play a role. Additionally, Si–Si–O unit can participate. For example, the longest wavelength absorption of 1,1,1-trimethoxy-2,2,2-trimethyldisilane, $(MeO)_3SiSiMe_3$, occurs at 234 nm in markedly contrast with 1,1,2-isomer, $(MeO)_2MeSiSiMe_2OMe$ (207 nm) [15]. The UV properties of silsesquioxanes have not been studied much; further investigation including the comparison with other octasilsesquioxanes are now in progress.

In summary, we determined the crystal structure of $(t\text{-}BuMe_2SiSi)_8$ **1**. Taking advantage of its high reactivity, we synthesized octakis(*tert*-butyldimethylsilylsilsesquioxane) **3** by the peracid oxidation. As the first example of the octasilsesquioxane with bulky substituents, **3** showed some alluring physical properties.

Table 3
Selected bond lengths (Å) and angles (°) for 3

Bond lengths					
Si(1)–O(1)	1.620(7)	Si(1)–O(2)	1.621(6)	Si(1)–O(3)	1.622(7)
Si(2)–O(1)	1.628(7)	Si(2)–O(4)	1.625(6)	Si(2)–O(5)	1.627(6)
Si(3)–O(2)	1.630(6)	Si(3)–O(6)	1.626(3)	Si(4)–O(3)	1.627(6)
Si(4)–O(7)	1.626(4)	Si(1)–Si(11)	2.344(4)	Si(2)–Si(22)	2.352(5)
Si(3)–Si(33)	2.349(4)	Si(4)–Si(44)	2.356(4)	Si(11)–C(11)	1.880(16)
Si(11)–C(12)	1.862(16)	Si(11)–C(13)	1.889(13)	Si(22)–C(21)	1.891(20)
Si(22)–C(22)	1.903(20)	Si(22)–C(23)	1.864(16)	Si(33)–C(31)	1.885(14)
Si(33)–C(32)	1.876(13)	Si(33)–C(33)	1.900(12)	Si(44)–C(41)	1.878(14)
Si(44)–C(42)	1.879(15)	Si(44)–C(43)	1.896(13)		
Bond angles					
Si(1)–O(1)–Si(2)	149.8(4)	Si(1)–O(2)–Si(3)	148.5(4)	Si(1)–O(3)–Si(4)	152.2(4)
O(1)–Si(1)–O(2)	109.2(3)	O(1)–Si(1)–O(3)	108.2(3)	O(2)–Si(1)–O(3)	108.7(3)
O(1)–Si(2)–O(4)	107.7(3)	O(1)–Si(2)–O(5)	109.4(3)	O(4)–Si(2)–O(5)	108.6(3)
O(2)–Si(3)–O(6)	107.9(3)	O(3)–Si(4)–O(7)	109.4(3)	O(1)–Si(1)–Si(11)	111.3(3)
O(2)–Si(1)–Si(11)	110.4(2)	O(3)–Si(1)–Si(11)	109.0(2)	O(1)–Si(2)–Si(22)	106.0(3)
O(4)–Si(2)–Si(22)	116.0(3)	O(5)–Si(2)–Si(22)	109.0(3)	O(2)–Si(3)–Si(33)	109.3(2)
O(6)–Si(3)–Si(33)	112.5(3)	O(3)–Si(4)–Si(44)	107.9(3)	O(7)–Si(4)–Si(44)	113.4(3)
Si(1)–Si(11)–C(11)	108.7(5)	Si(1)–Si(11)–C(12)	107.3(5)	Si(1)–Si(11)–C(13)	111.6(4)
Si(2)–Si(22)–C(21)	109.6(6)	Si(2)–Si(22)–C(22)	105.7(6)	Si(2)–Si(22)–C(23)	114.0(5)
Si(3)–Si(33)–C(31)	110.5(5)	Si(3)–Si(33)–C(32)	106.4(4)	Si(3)–Si(33)–C(33)	111.3(4)
Si(4)–Si(44)–C(41)	108.8(5)	Si(4)–Si(44)–C(42)	106.3(5)	Si(4)–Si(44)–C(43)	112.4(5)

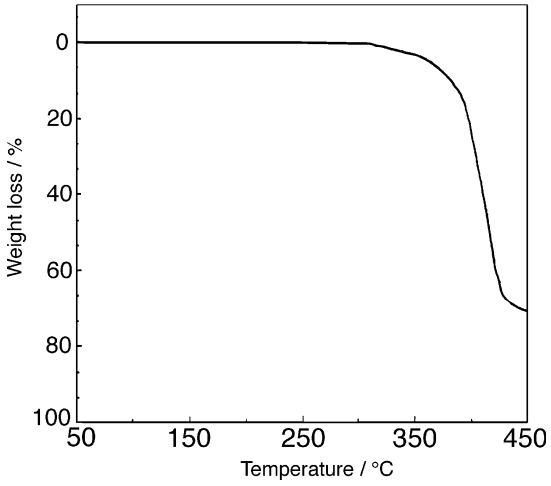

Fig. 4. Thermogravimetric curves of **3**.

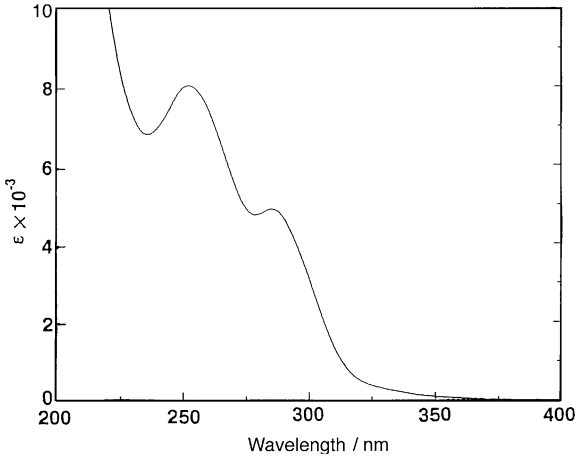

Fig. 5. UV–vis spectra of **3** in cyclohexane.

3. Experimental

The solid state ^{13}C and ^{29}Si magic angle spinning (MAS) NMR spectra were measured on a JEOL GX-270 spectrometer using a standard ^{1}H cross-polarization technique at 67.8 and 53.5 MHz, respectively. Samples were observed in rotors at spinning rates of 5.8–6.2 kHz. The solid ^{13}C and ^{29}Si chemical shifts were based on hexamethylbenzene and polydimethylsilane as an external standard. Electronic absorption spectra were recorded on a JASCO Ubest-50 spectrometer. IR spectra were measured with a JASCO A-102 spectrometer. Mass spectra were taken on a JEOL JMS-DX302 instrument. Thermogravimetric analyses were obtained on a Rigaku THERMOFLEX TG-8110 with a Rigaku Thermal Analysis Station TAS-100 instrument under Ar atmosphere.

3.1. X-ray crystallography of octakis(tert-butyldimethylsilyl)pentacyclo[4.2.0.0^{2,5}.0^{3,8}.0^{4,7}]-octasilane (*1*)

Yellow plate crystals of **1** were obtained by slow evaporation from the methylcyclohexane solution at r.t. All measurements were made on a Rigaku RAXIS-IV imaging plate are detector with graphite monochromated Mo–Kα radiation. Indexing was performed from three oscillations which were exposed for 4.0 min. The data were collected at a temperature of 20 ± 1 °C to a

maximum 2θ value of 55.1°. A total of 4 of 6° oscillation images were collected, each being exposed for 4.0 min. The crystal-to-detector distance was 105.0 mm with the detector at the zero swing position. Readout was performed in the 0.100 mm pixel mode. The data were corrected for Lorenz and polarization effects. The structure was solved by SHELXS-86 [16] and expanded using Fourier techniques. Hydrogen atoms were included but not refined. The final cycle of full-matrix least-squares refinement was based on 5209 observed reflections ($I > 4.00\sigma(I)$) and 513 variable parameters and converged.

3.2. Peracid oxidation of octasilacubane *1*

To a solution of **1** (122 mg, 0.11 mmol) in benzene (30 ml) was added *m*-chloroperbenzoic acid (265 mg, 1.54 mmol) in benzene (20 ml) at r.t. The yellow color of **1** gradually faded. After being stirred for 7 days, the reaction mixture was evaporated. Fractional crystallization from ethanol provided colorless microcrystals of **3** (140 mg, 98%). 1,3,5,7,9,11,13,15-Octakis(*tert*-butyldimetylsilyl)pentacyclo[9.5.1.1^{3,9}.1^{5,15}.1^{7,13}]octasiloxane (**3**): colorless prisms; m.p. 300 °C (dec.); ^{1}H-NMR ($CDCl_3$) δ 0.94 (s, 72H), 0.04 (s, 48H) ppm.; ^{13}C-NMR ($CDCl_3$): δ 27.84, 16.61, −6.20 ppm; ^{29}Si-NMR ($CDCl_3$): δ −12.67, −71.31 ppm; ^{13}C-NMR (CP-MAS) δ 28.82, 17.65, −4.91, −5.85 ppm; ^{29}Si-NMR (CP-MAS) δ −11.20, −12.90, −70.76; UV (cyclohexane) λ_{max} (ε) 250 (8000), 285 (4900) nm; IR (KBr) ν 2961 (s), 2943 (s), 2899 (s), 2859 (s), 1470 (s), 1445 (w), 1413 (w), 1367 (m), 1258 (m), 1247 (m), 1080 (s), 1008 (m), 940 (w), 835 (s), 823 (s), 806 (s) cm^{-1}; MS (70 eV) *m*/*z* 1336 (M^+, isotope pattern coefficient of 68%), 1137 (75), 1138 (100), 1139 (64), 1140 (49), 1141 (29); Anal. Calc. for $C_{48}H_{120}Si_{16}O_{12}$: C, 43.06; H, 9.03. Found: C, 43.31; H, 8.91%.

3.3. X-ray crystallography of *3*

Crystals of **2** suitable for X-ray analysis were obtained by recrystallization from a methylcyclohexane solution. Intensity data for **2** were collected on a Enraf–Nonius CAD-4 diffractometer using graphite monochromated Cu–Kα radiation at r.t. The structures was solved by direct methods with MULTAN-78 program [17] using the reflections with $|F_o| \geq 3\sigma(F_o)$. The structures was refined anisotropically for non-hydrogen atoms by full-matrix least-squares and hydrogen atoms were not refined.

Acknowledgements

This work was support by a grant from the Ministry of Education, Culture, Sports, Science and Technology of Japan (Grant-in-Aid No. 12640510) for M.U. and CREST-JST.

References

[1] (a) A. Sekiguchi, H. Sakurai, Adv. Organomet. Chem. 37 (1995) 1;
(b) A. Sekiguchi, S. Nagase, in: S. Patai, Z. Rappoport (Eds.), The Chemistry of Organic Silicon Compounds, vol. 2 (and references cited therein), John Wiley & Sons, Chichester, 1998, pp. 119–152 (and references cited therein);
(c) A. Sekiguchi, T. Yatabe, H. Kamatani, C. Kabuto, H. Sakurai, J. Am. Chem. Soc. 114 (1992) 6260;
(d) K. Furukawa, M. Fujino, N. Matsumoto, J. Organomet. Chem. 515 (1996) 37 (and reference 3).
[2] H. Matsumoto, K. Higuchi, Y. Hoshino, H. Koike, Y. Naoi, Y. Nagai, J. Chem. Soc. Chem. Commun. (1988) 1083.
[3] H. Matsumoto, K. Higuchi, S. Kyushin, M. Goto, Angew. Chem. Int. Ed. Engl. 31 (1992) 1354.
[4] M. Unno, K. Higuchi, M. Ida, H. Shioyama, S. Kyushin, H. Matsumoto, M. Goto, Organometallics 13 (1994) 4633.
[5] M. Unno, H. Shioyama, M. Ida, H. Matsumoto, Organometallics 14 (1995) 4004.
[6] M. Unno, T. Yokota, H. Matsumoto, J. Organomet. Chem. 521 (1996) 409.
[7] Y. Kanemitsu, K. Suzuki, S. Kyushin, H. Matsumoto, Phys. Rev. B 51 (1995) 13103.
[8] H. Horiuchi, Y. Nakano, T. Matsumoto, M. Unno, H. Matsumoto, H. Hiratsuka, Chem. Phys. Lett. 322 (2000) 33.
[9] M. Unno, K. Higuchi, K. Furuya, H. Shioyama, S. Kyushin, M. Goto, H. Matsumoto, Bull. Chem. Soc. Jpn. 73 (2000) 2093.
[10] S. Nagase, Pure Appl. Chem. 65 (1993) 675.
[11] A.R. Bassindale, P.G. Tayler, in: S. Patai, Z. Rappoport (Eds.), The Chemistry of Organic Silicon Compounds, Wiley, Chichester, 1989, p. 895.
[12] M. Unno, B.A. Shamsul, H. Saito, H. Matsumoto, Organometallics 15 (1996) 2413.
[13] (a) M.A. Hossain, M.B. Hursthouse, K.M.A. Malik, Acta Crystallogr. B 35 (1979) 2258;
(b) K. Larsson, K. Ark. Kemi. 16 (1980) 203;
(c) V.W. Day, W.G. Klemperer, V.V. Mainz, M. Miller, J. Am. Chem. Soc. 107 (1985) 8262;
(d) F.J. Feher, T.A. Budzichowski, J. Organomet. Chem. 373 (1989) 153;
(e) M. Unno, K. Takada, H. Matsumoto, Chem. Lett. (1998) 489.
[14] U. Dittmar, B.J. Hendan, U. Flörke, H.C. Marsmann, J. Organomet. Chem. 489 (1995) 185.
[15] E. Hengge, N. Holtschmidt, Monatshefte für Chemie 99 (1964) 340.
[16] SHELXS-86, G.M. Sheldrick, Crystallographic Computing 3, Oxford University Press, 1985.
[17] MULTAN-78, A system of Computer Programs for the Automatic Solution of Crystal Structures from X-ray Diffraction Data; University of York, England and Louvain, Belgium, 1978.